A R C H I V E S O F M E T A L L U R G Y A N D M A T E R I A L S
Volume 57 2012 Issue 4
DOI: 10.2478/v10172-012-0116-2

J. RYŚ*, A. ZIELIŃSKA-LIPIEC*

DEFORMATION OF FERRITE-AUSTENITE BANDED STRUCTURE IN COLD-ROLLED DUPLEX STEEL

ODKSZTAŁCENIE PASMOWEJ STRUKTURY FERRYTU I AUSTENITU W WALCOWANEJ NA ZIMNO STALI DUPLEX

Duplex type ferritic-austenitic stainless steels develop a specific two-phase banded structure upon thermo-mechanical pre-treatment and subsequent cold-rolling. The band-like morphology of ferrite and austenite imposes different conditions on plastic deformation of both constituent phases in comparison to one-phase ferritic and austenitic steels.

In the present research the ingot of a model ferritic-austenitic steel of duplex type, produced by laboratory melt, was subjected to preliminary thermo-mechanical treatment including forging and solution annealing. Afterwards cold-rolling was conducted over a wide deformation range. The investigations comprised examination of ferrite and austenite microstructures by means of optical and transmission electron microscopy and texture measurements after selected rolling reductions.

The presented results indicate that deformation mechanisms operating within the bands of both constituent phases are essentially the same as compared to one-phase steels, however their appearance and contribution are changed upon deformation of two-phase banded structure. Different deformation behavior within ferrite-austenite bands in duplex steels, visible especially at higher strains, considerably affects microstructure evolution and in consequence texture formation in both phases.

Keywords: duplex stainless steel, two-phase banded structure, deformation mechanisms, ferrite and austenite microstructure, rolling textures

Podczas wstępnej obróbki cieplno-plastycznej i dalszego walcowania na zimno w nierdzewnych stalach ferrytyczno-austenitycznych typu duplex następuje rozwój charakterystycznej pasmowej struktury dwufazowej. Pasmowa morfologia ferrytu i austenitu stwarza odmienne warunki dla procesu odkształcenia plastycznego obu składowych faz w porównaniu do jednofazowych stali ferrytycznych i austenitycznych.

W prezentowanych badaniach wlewek modelowej stali ferrytyczno-austenitycznej typu duplex, uzyskany na drodze wytopu laboratoryjnego, poddano wstępnej obróbce cieplno-plastycznej obejmującej kucie na gorąco i przesycanie. Następnie przeprowadzono walcowanie na zimno w szerokim zakresie deformacji. Badania obejmowały obserwacje mikrostruktury ferrytu i austenitu za pomocą mikroskopii optycznej i transmisyjnej mikroskopii elektronowej oraz pomiary tekstury po wybranych stopniach odkształcenia.

Prezentowane wyniki wskazują, że mechanizmy odkształcenia działające w obszarach obu składowych faz są zasadniczo takie same jak w przypadku stali jednofazowych, jednakże ich udział i znaczenie ulegają istotnym zmianom podczas odkształcenia pasmowej struktury dwufazowej. Odmienny sposób odkształcenia pasm ferrytu i austenitu w stalach duplex, widoczny zwłaszcza w zakresie większych odkształceń, wpływa w istotny sposób na rozwój mikrostruktury a w konsekwencji na tworzenie się tekstury w obu fazach.

1. Introduction

In recent decades, duplex type ferritic-austenitic stainless steels attracted continuously growing interest from industry and research laboratories due to a beneficial combination of mechanical properties and corrosion resistance [1-10]. Technological processes for a major part of products manufactured of ferritic-austenitic stainless steels include hot- and subsequent cold-plastic working. During rolling of duplex steel plates and sheets both component phases are plastically deformed and develop a specific band-like structure [1-7]. A complex character of deformation processes in duplex steels results not only from two-phase structure, but first of all is a consequence of ferrite and austenite morphology with (α/γ) phase interfaces oriented for the most part parallel to the rolling plane. From a number of previous research works it results that major deformation mechanisms operating within the areas of both phases are essentially the same as in one-phase steels. It is expect-

* AGH UNIVERSITY OF SCIENCE AND TECHNOLOGY, DEPARTMENT OF PHYSICAL AND POWDER METALLURGY, 30-059 KRAKÓW, 30 MICKIEWICZA AV., POLAND

ed however that their contribution and appearance may considerably change upon deformation of duplex type ferritic-austenitic steels [1-8]. This particularly concerns mechanisms controlling deformation behavior at higher strains, i.e. starting from the range corresponding to macroscopic strain localization in one-phase steels [6-8]. The band-like ferrite-austenite morphology may additionally exert a significant influence on texture formation in both constituent phases. Depending on chemical composition, initial orientation distributions as well as conditions of thermo-mechanical pre-treatment and further cold-rolling deformation textures in duplex steels frequently differ from those in one-phase ferritic and austenitic steels [3-7].

The main purpose of the present research was the analysis of microstructure evolution and texture formation in model ferritic-austenitic duplex type steel subjected to cold-rolling within a wide deformation range, up to 90% of reduction, taking into account specific initial textures of ferrite and austenite after the preliminary treatment.

2. Material and experimental procedure

The material investigated in the present research was a model laboratory melt of the ferritic-austenitic steel X1CrNi24-6, without additions of molybdenum, nitrogen, etc. The chemical composition of the steel under examination (given in Table 1) assured the phase constitution of duplex type after standard thermo-mechanical pre-treatment and allowed to compare its deformation behavior with highly alloyed commercial grades of modern duplex steels.

TABLE 1

Chemical composition of the examined duplex steel in wt%

C	Cr	Ni	Mn	Si	Al	S	P	N	Fe
0.009	23.7	6.0	1.23	0.34	<0.020	0.010	<0.008	0.012	bal.

The steel ingot was industrially homogenized and forged within the temperature range 1100÷900°C. Afterwards the rectangular steel rods cut-out of the ingot were annealed at the temperature 1100°C for 3 hours and quenched in the water. After solution treatment the steel rods were subjected to reversed rolling at ambient temperature within the range up to 90% of thickness reduction (ε =2.3). Cold-rolling was carried out parallel to the direction of hot deformation, with the ratio (L_c/h_m) ⩾ 1.0, to avoid a strain gradient over the thickness of the sheet in each roll pass; where $L_c = \sqrt{R\Delta h}$ – the length of the arc of contact, R – radius of rolls, Δh – thickness reduction per pass and h_m – the mean thickness of the sheet [5].

Observations of the ferrite-austenite two-phase morphology after preliminary thermo-mechanical treatment and upon subsequent cold-rolling were conducted by means of optical microscopy (Neophot-2 and Axiovert-200 MAT). Examination of the ferrite and austenite microstructures after selected rolling reductions and the analysis of deformation mechanisms within the bands of both constituent phases were carried out by means of transmission electron microscopy (JEM200CX and Tecnai G2 F20) on thin foils prepared from the longitudinal (ND-RD) sections of the rolled sheets.

X-ray investigations were conducted by means of Bruker diffractometer D8 Advance, using $Co_{K\alpha}$ radiation ($\lambda_{K\alpha}$ =0,179nm). X-ray examination included texture measurements from the centre layers of the rolled sheets, for the initial state and after successive rolling reductions. Texture analysis based on the orientation distribution functions (ODFs) calculated from experimental pole figures recorded of three planes for each of the constituent phases, i.e. the {110}, {100} and {211} planes for the bcc α-phase and the {111}, {100} and {110} planes for the fcc γ-phase.

3. Results and discussion

3.1. Starting texture and microstructure

Initial orientation distribution is one of the essential factors determining deformation behavior of polycrystalline material upon further plastic working. Texture measurements conducted after the preliminary thermo-mechanical treatment revealed well-defined initial textures in both constituent α- and γ-phases. The ferritic α-phase exhibited relatively strong cubic texture with the maximum intensity f(g)=9.8. The dominant texture component, i.e. the {100}<001>orientation, was detected on the background of nearly random texture. The strongest texture component of the austenitic γ-phase was the {110}<001> Goss orientation, having the intensity f(g)=5.5 (Fig.1a). The initial texture of austenite was sharp however relatively week. According to Bain relationship, the 45° rotation of the {100}<001>cubic orientation around the successive <100>axes leads to the rotated cubic {100}<011>, Goss {110}<001>or rotated Goss {110}<011>orientations. Hence the crystallographic relation between the strongest components of the ferrite and austenite initial textures may be described by one of the orientation variants from Bain relationship (Fig.1b): $[001]\gamma \parallel [001]\alpha$; $[1\bar{1}0]\gamma \parallel [100]\alpha$; $[110]\gamma \parallel [010]\alpha$ [5].

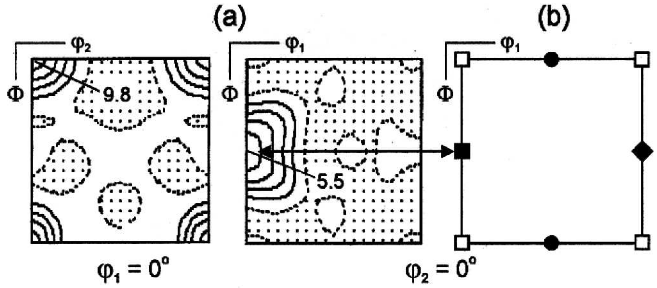

Fig. 1. The textures of ferrite and austenite after preliminary treatment in sections ϕ_1 =0° and ϕ_2 =0° respectively **(a)** and the orientation variants from Bain relationship **(b)**

The initial textures in both α- and γ-phases resulted from the applied thermo-mechanical treatment which comprised the process of forging. The occurrence of strong {100}<001>cubic texture within the ferritic phase after hot deformation of duplex stainless steel was reported by Keichel et al. [1] for the case of rod-materials subjected to forging. As compared to rolling, there is a different strain path in the course of forging with compressive stresses altering between normal and transverse direction of a rod. On the other hand, the comparison of the austenite textures for rod-materials with those for sheet-materials after hot-rolling indicates at strong intensities of the {110}<001> Goss orientation in duplex steels after forging [1].

The morphology of the ferrite and austenite two-phase structure after the preliminary treatment resulted from the applied hot plastic working, i.e. forging, and changed only insignificantly upon the subsequent solution treatment at the temperature 1100°C. Based on the metallographic analysis conducted after the solution treatment the volume fraction of ferrite (V_v^F) was estimated at about 60%. Hence the ferritic α-phase was more continuous and constituted a matrix with islands of the austenitic γ-phase. On the longitudinal sections of the forged rod the areas of austenite were elongated parallel to the rod axis, i.e. direction of plastic flow, but on the cross-section the austenite grains were nearly equiaxed [5]. Microstructure like this was subsequently subjected to cold-rolling parallel to the direction of hot-working.

3.2. Rolling texture development

The strongest components from the ferrite and austenite initial textures, i.e. the {100}<001> cubic and the {110}<001> Goss orientations respectively, appeared relatively stable orientations in the course of cold-rolling over a wide deformation range, up to 60-70% of reduction (Figs. 2a,b).

Texture changes of the austenitic γ-phase upon rolling occurred comparatively small. The {110}<001> Goss orientation remained a dominant component of the austenite texture within the whole range of deformations, i.e. up to 90% of reduction (ε = 2,3). The only changes refer to texture spread along the α =<110>|| ND and η =<001>|| RD fibers and visible weakening of texture intensity starting from 70% and 80% of deformation respectively (Fig. 2b). Up to this strain range texture components from the limited α-fibre (<110>|| ND), e.g.: the {110}<113> and the alloy type {110}<112> orientations, which are typical for one-phase austenitic steels, were nearly absent or showed very small intensities. Comparison of the rolling texture evolution in some duplex steels and one-phase austenitic steels by other authors (e.g. [3,7,11]) also indicates at higher intensities of Goss orientation in the case of duplex materials.

Despite the fact that the cubic orientation is not a typical one for the rolling textures of ferritic steels [12], it remained a dominant texture component within the texture of the α-phase up to about 70% of deformation. Simultaneously, the orientation {100}<001> showed relatively high texture intensities within the range f(g)=12.5-14.0 (Fig. 2a). Starting from about 80% of deformation the rolling texture of ferrite became visibly weaker. The strongest texture component was changed to the {100}<011> rotated cubic orientation with the maximum intensity f(g)=6.9. The texture of ferrite at this strain level may be described by the non-homogeneous ε-fibre (<001>|| ND) and the limited α_1-fibre (<110>|| RD). After 90% of rolling reduction the texture maximum was shifted along Φ direction into the range {111}<011>to {112}<011> and the texture intensity reduced to f(g)=5.1. At higher strains the texture of ferrite was described by the limited and non-homogeneous α_1-fibre and weak ε-fibre (Fig. 2a). It should be noted that the γ-fiber (<111>|| ND), which is a typical orientation fiber for the rolling textures of one-phase ferritic steels, was absent within the texture of the α-phase and appeared not before 80% of rolling reduction (Fig. 2a).

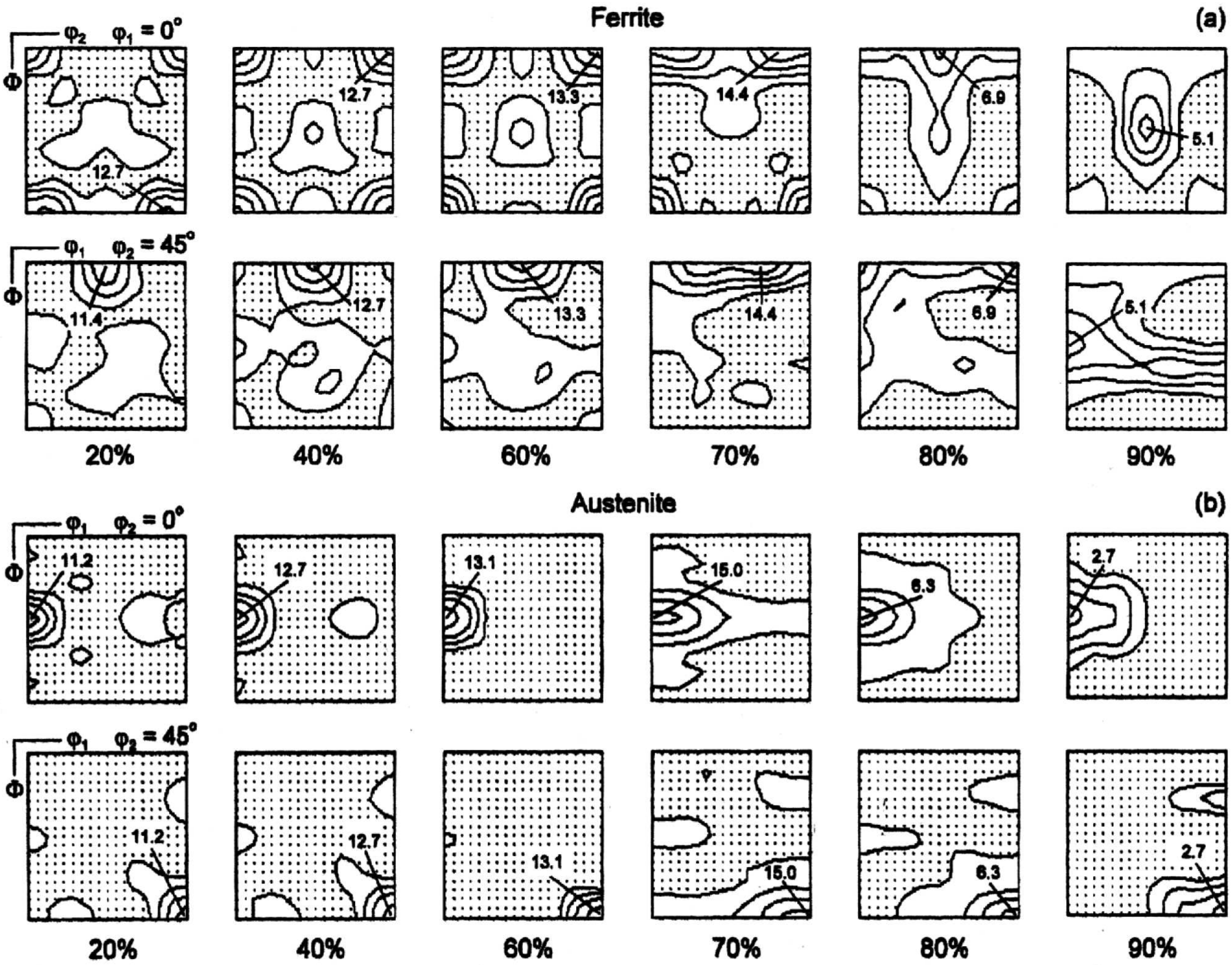

Fig. 2. Orientation distribution functions (ODFs) in sections ϕ_1 =0°, ϕ_2 =45° for ferrite **(a)** and in sections ϕ_2 =0°, ϕ_2 =45° for austenite **(b)** after the selected rolling reductions.

3.3. Deformation microstructure

Cold-rolling was carried out after the preliminary thermo-mechanical treatment parallel to the direction of hot-deformation. Both constituent phases were plastically deformed in the course of rolling and developed a characteristic band-like structure consisting of alternate bands of ferrite and austenite aligned parallel to the rolling plane, so-called *pancake* structure. With increasing rolling reduction a significant refinement of the two-phase structure was observed. At higher strains the thickness of a number of austenite bands was reduced much below one micrometer. The bands of ferrite were usually thicker and showed more continuous character due to the phase composition of the steel after solution treatment. Changes in morphology of the ferrite-austenite microstructure on the longitudinal section (ND-RD) of the rolled sheet after 30-70% of reduction are shown in Figures 3a-c. Starting from about 70-80% of deformation the structural effects in the form of folds and offsets were observed within the two-phase banded structure. These characteristic features resulted from strain localization i.e. local shearing, which intersects at least several ferrite and austenite bands (Figs. 3c, 11a).

Within the range of medium strains the process of plastic deformation in austenitic stainless steels usually proceeds by combination of two deformation mechanisms, i.e.: slip and twinning. The relative contribution of both mechanisms depends on several factors including; stacking fault energy (SFE), crystallographic orientation and deformation conditions. Owing to the chemical composition of the examined duplex steel, without addition of nitrogen (Table 1), the SFE value of the austenitic γ-phase was estimated as medium, that is why mechanical twinning did not become a major deformation mechanism [2,10]. Microstructure observations conducted after small and medium rolling reductions indicate that austenite was deformed mainly by planar slip of dissociated dislocations (Fig. 4) and deformation twins appeared occasionally, only in some favorably oriented grains (Fig. 5a-d). Microstructures within the austenite areas after 50% of rolling reduction (Fig. 6) show two sets of mutually intersecting coarse slip bands aligned parallel to $(11\bar{1})$ and $(1\bar{1}1)$ slip planes. In places of their intersections clear offsets are visible, which resulted from mutual shearing. With increasing strain up to 70% of deformation a further development of this type of strain localization was observed, with structural effects limited to the areas (bands) of the γ-phase (Fig. 9).

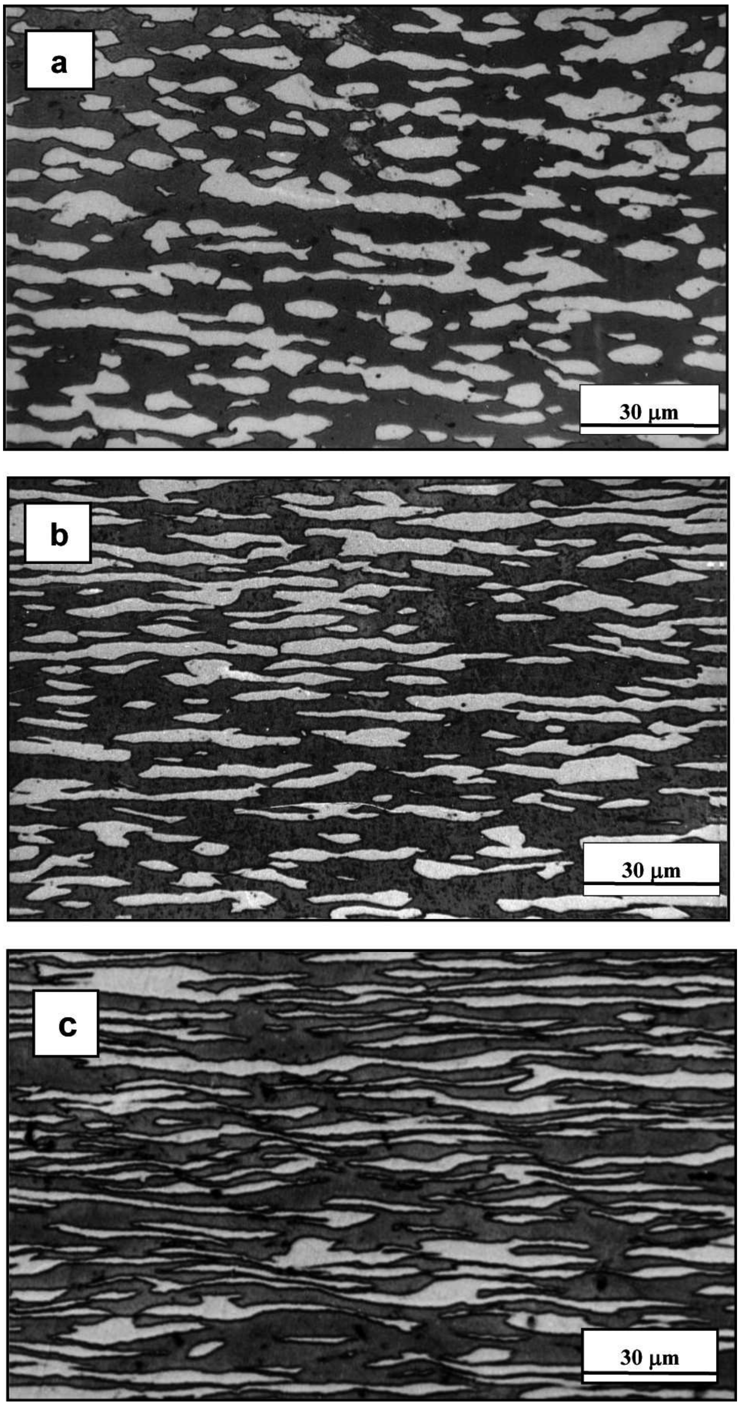

Fig. 3. Morphology of the (α/γ) two-phase structure after 30, 50 and 70% of deformation

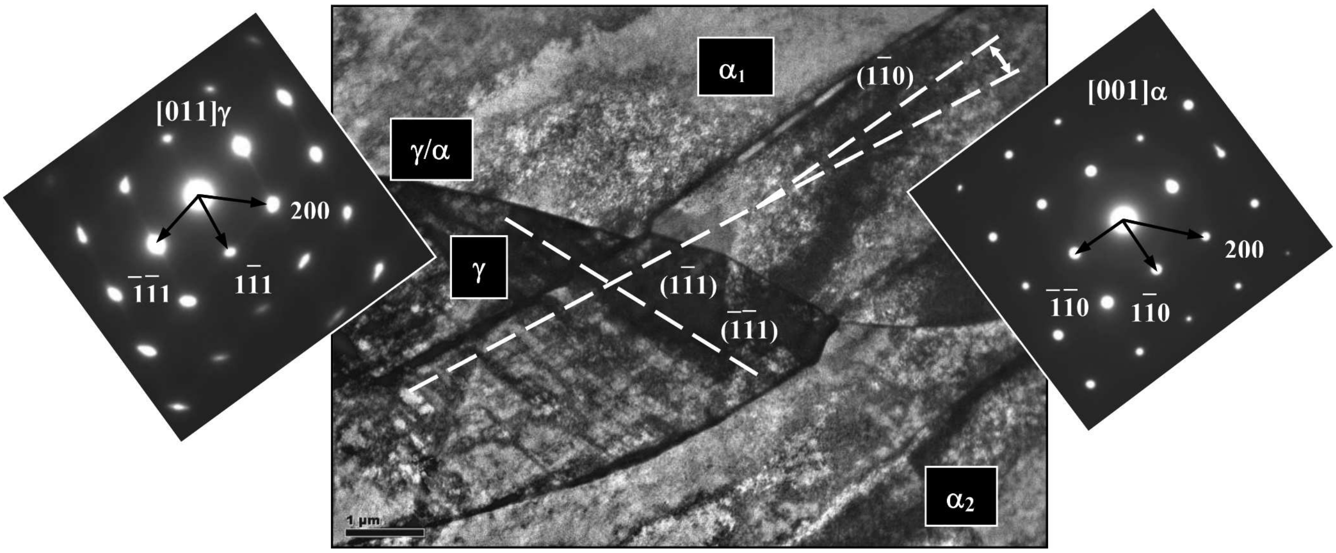

Fig. 4. Ferrite and austenite microstructure after 30% of rolling reduction

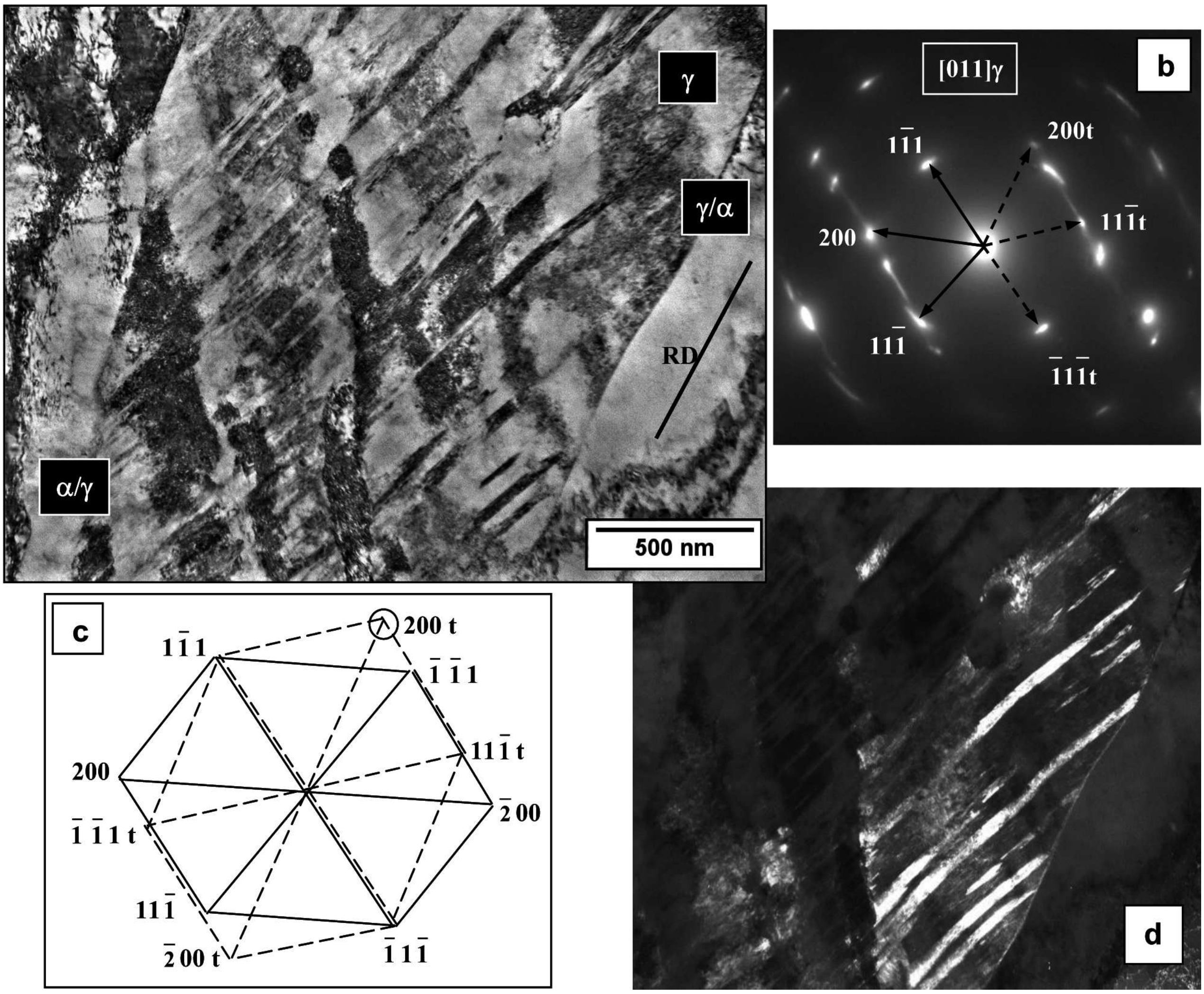

Fig. 5. Micro-bands within the austenite area showing twin relation with respect to matrix after 50% of deformation

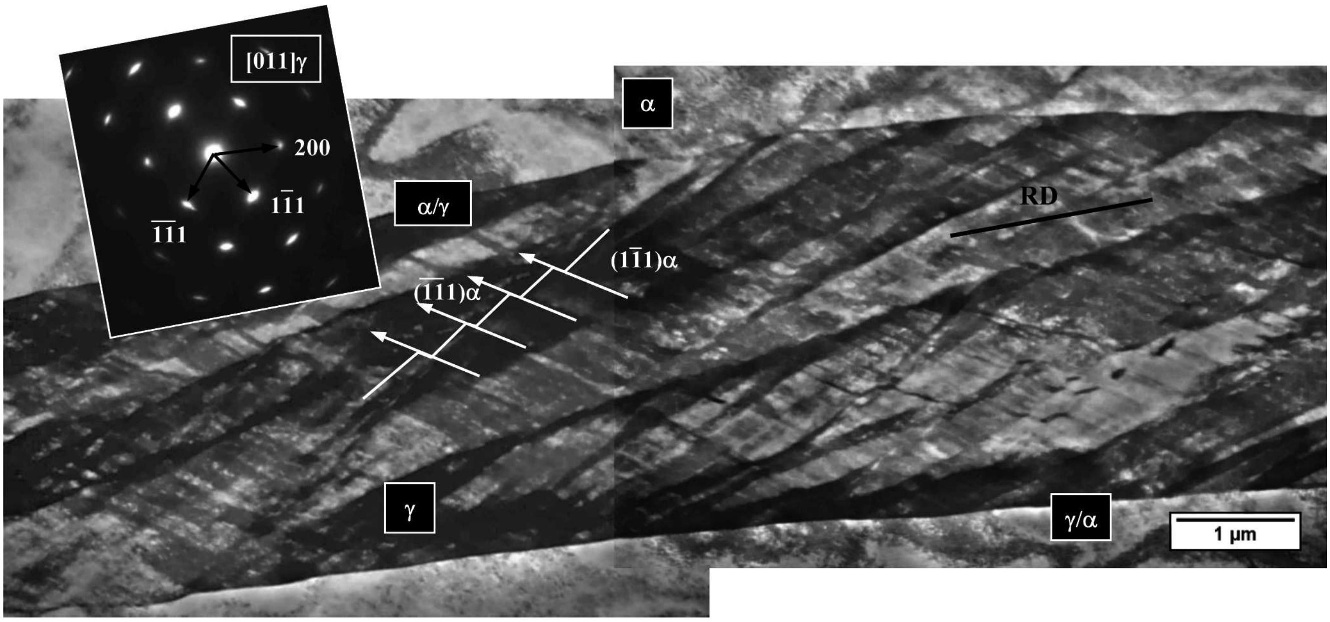

Fig. 6. Microstructure within a band of austenite, with two sets of mutually intersecting slip bands from {111}planes, after 50% of reduction

The microstructures of the ferritic α-phase observed at medium strains displayed a conventional cold-worked substructure with micro-bands of increased dislocation density aligned parallel to the two sets of slip planes symmetrical with respect to the (α/γ) interface. At about 50% reduction these micro-bands consisted of dislocation cell segments separated by dense dislocation walls (Fig. 7) and formed the ribbon-like substructure at about 70% of deformation (Fig. 9). Likewise in the case of austenite the micro-bands observed within the ferrite areas showed offsets or folds due to the mutual intersections. These effects resulted from micro-shearing, which mainly corrugates the ribbon-like ferrite substructure and in consequence leads to the formation of a wavy lamellar structure. That is why the overall directions of micro-bands were frequently not parallel to {110}slip planes.

In order to clarify a deformation behavior of both phases in the course of cold-rolling, calculations of the relative shear stresses (i.e. the ratios m = τ/σ) for the strongest texture components were conducted. For the case of the ferritic α-phase the {100}<001>cubic orientation was the strongest texture component up to 60% of reduction. Calculations of the ratio m = τ/σ showed that the highest values of the relative shear stresses (m = 0,816) were in four slip systems and deformation of ferrite could proceed in two slip planes, (101) and (10$\bar{1}$), which were symmetrical in relation to <001>|| RD (Fig. 8a). Similarly, deformation of the austenitic γ-phase, with the strongest Goss component {110}<001>, could proceed by operation of four equally stressed slip systems, having the same values of the relative shear stresses (m=0,816). Also in this case the two active slip planes, i.e. the (111) and (11$\bar{1}$), were symmetrical with respect to the rolling direction <001>|| RD (Fig. 8b). Hence, the microstructures observed within adjacent bands of ferrite and austenite at medium strains resulted from the operation of four slip systems in each phase symmetrical in relation to RD with equal values of the relative shear stresses (Figs. 8a,b). It should be noted however, that not all of the most stressed slip systems need to operate simultaneously and usually their activation is sequential, so as to enable plastically compatible deformation of both component phases. Such slip behavior in examined duplex steel, without significant lattice rotations, resulted in texture stability within ferrite and austenite bands over a relatively wide deformation range, i.e. up to about 60-70% of rolling reduction.

Burgers vectors of glide dislocations in the bcc α-phase and the fcc γ-phase are obviously different ($\bar{b}_\alpha$ =a/2<111>and $\bar{b}_\gamma$ =a/2<110>), that is why only slip transfer may occur across the (α/γ) interfaces at low and medium strains [13]. In general the rules determining slip transmission across grain boundaries in one-phase materials can be employed to the co-deformation of two-phase alloys [13,14]. Furthermore it occurs, that these conditions apply not only for the case of bcc/fcc structures that exhibit K-S orientation relation [14] but also for the case of Bain relationship, as was shown in tensile tested (α/γ) duplex steel bicrystals by the present author [13]. It means that for compatible deformation of the bcc and fcc phases their slip planes not necessarily have to be parallel and the essential requirement seems to be compatibility of plastic strains in adjacent crystals.

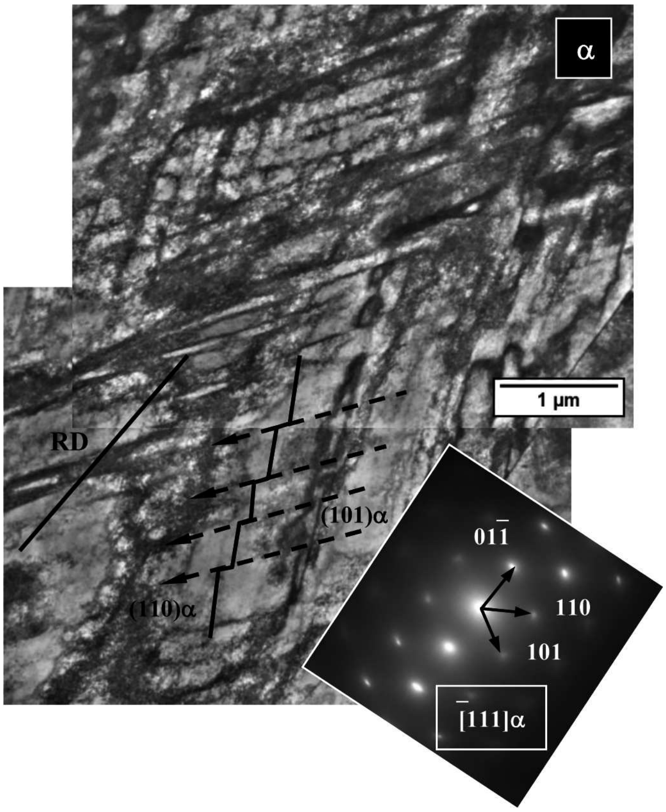

Fig. 7. Microstructure within a band of ferrite after 50% of deformation typical for medium strains

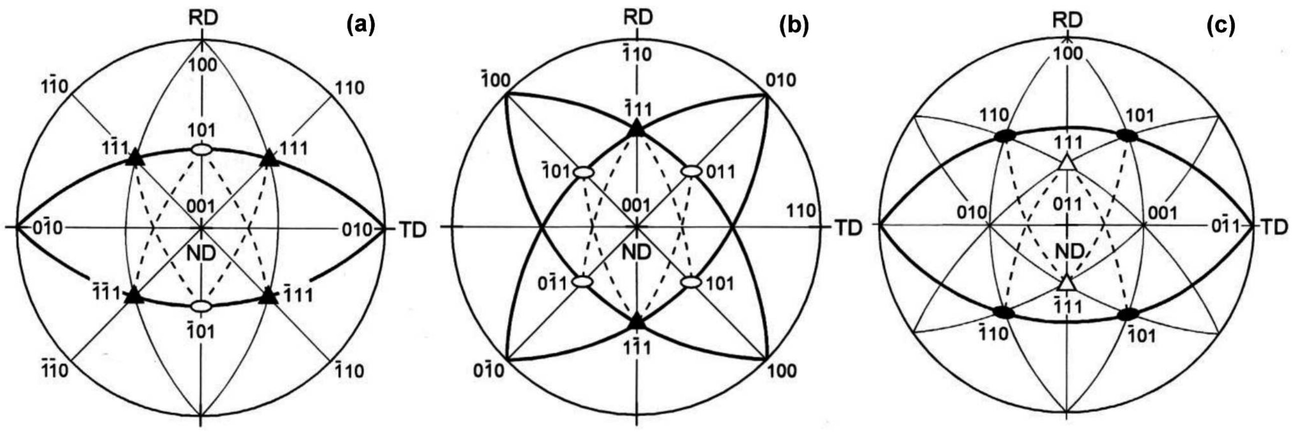

Fig. 8. Stereographic projections showing the most stressed slip systems for the dominant texture components in ferrite **(a, b)** and in austenite **(c)**

During deformation of ferritic-austenitic duplex steels both component phases mutually hinder their deformation. Due to the requirement of strain accommodation at the (α/γ) interfaces the dislocation density considerably increases upon cold-rolling deformation [2,8]. It is expected that increasing dislocation density and a considerable refinement of two-phase structure at higher strains force activation of subsequent slip systems. In the case of the ferritic α-phase a change of slip plane is much easier as compared to austenite. This very likely accounts for a change of the major component within the ferrite texture, which is shifted to the {100}<011>rotated cubic orientation within the range 60-80% of deformation (Fig.2a). In the case of the {100}<011>orientation component the values of the relative shear stresses are also the same (m = 0,816) in four slip systems symmetrical with respect to RD (Fig.8c). Moreover additional deformation mechanisms frequently appear at higher strains [2,8]. From an energetic point of view the mechanisms such as mechanical twinning and deformation induced $(\gamma \rightarrow \alpha)$ transformation as well as shear band formation usually occur when conditions for deformation by slip are unfavorable. Due to the chemical composition of the steel under examination (Table 1) the austenite can be considered as a metastable phase with medium value of SFE [10]. That is why no evidence for twinning as a major deformation mechanism was found within the austenite bands. However, instability of the austenitic γ-phase and back-stresses from the surrounding ferrite matrix may result in the occurrence of deformation induced martensitic transformation upon further processing [2].

The microstructure inside the bands of the γ-phase started to change at higher strains, i.e. from about 70% of rolling reduction ($\varepsilon \geqslant 1{,}6$). Two bands of austenite visible in Figure 9 show relatively different microstructures from the view point of morphology. The band in the centre exhibits two intersecting sets of coarse slip bands, symmetrical with respect to the rolling direction, with visible offsets and folds resulting from mutual shearing. On the other hand the microstructure within the second band (on the right side) indicates at the occurrence of another mechanism of strain localization leading to formation of a single set of micro-bands. After 70% of deformation all these structural effects were still limited to the areas of austenite bands. Starting from about 80% of rolling reduction a strong refinement of the austenite microstructure was observed. These microstructures consisted of very thin band-like segments, which formed a lamellar-like substructure typical for higher strains

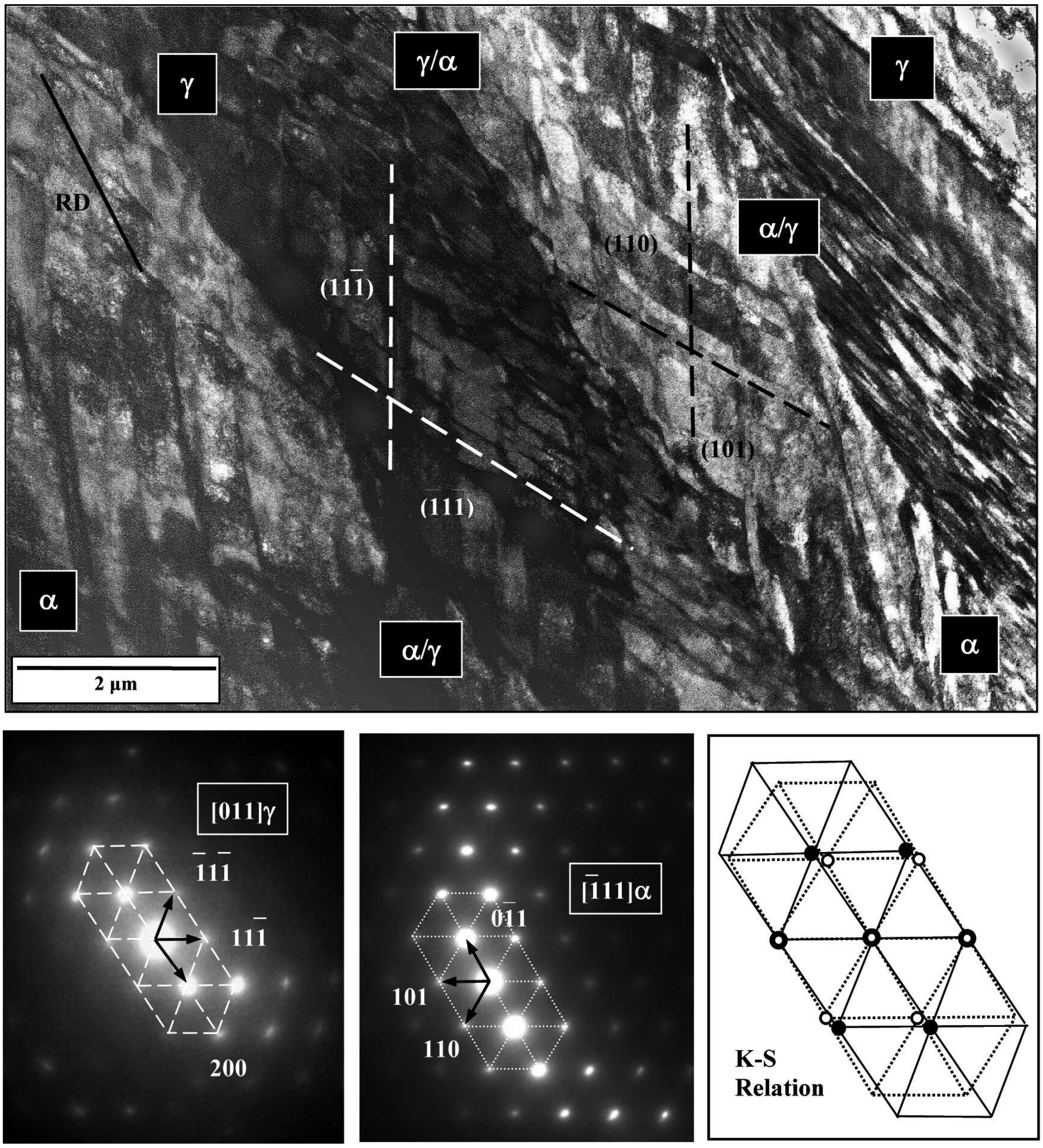

Fig. 9. Microstructures within the adjacent bands of ferrite and austenite after 70% of rolling reduction

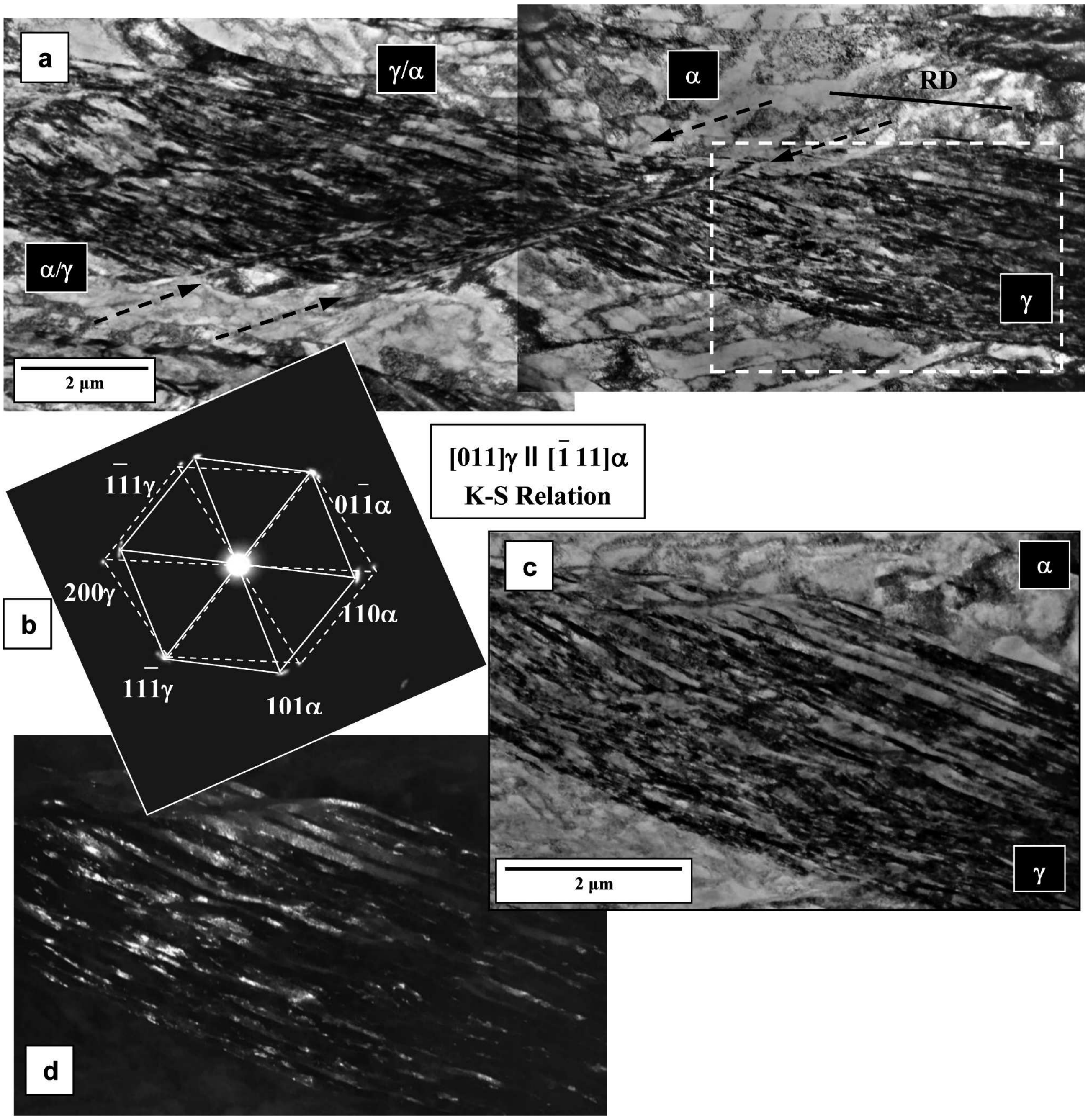

Fig. 10. Strongly refined lamellar-like microstructure within the austenite band after 80% of rolling reduction **(a, c)** and dark field analysis **(b, d)** indicating at ($\gamma \rightarrow \alpha$) transformation

(Fig. 10a,c). A considerable increase of dislocation density in microstructures of this type usually limits the homogeneous deformation and results in activation of another forms of strain localization. TEM observations revealed a development of micro-shear bands against a background of this lamellar-like substructure, which can be easily identified by corrugation of the austenite substructure (Fig. 10a). Additionally the dark field analysis conducted inside this austenite band (Fig. 10b,d) indicates that locally a certain part of the austenite underwent the strain induced ($\gamma \rightarrow \alpha$) transformation. Such deformation behavior within the bands of γ-phase explains the pronounced weakening and spread of the austenite rolling texture observed starting from the range 70-80% of reduction. Simultaneously TEM observations revealed some specific changes of microstructure which locally appeared inside the ferrite matrix at higher deformations. At about 80% of reduction a number of ferrite areas with high dislocation density clearly resemble partly recovered microstructures in the form of sub-grains elongated parallel to RD (Fig. 11), which very likely appeared due to the local occurrence of dynamic recovery. According to Foct and Akdut [2], when slip and/or mechanical twinning, local shear banding and martensitic transformation in the austenitic γ-phase are still not sufficient to accommodate the imposed external deformation, dynamic recovery within the ferritic α-phase takes place at higher strains. In duplex steel under examination these ferrite areas usually exhibited the {100}<001>cubic orientation, which was still present within the ferrite rolling texture even after 90% of reduction (Figs. 11, 2a).

Structural effects resulting from strain localization in the form of macroscopic shear bands usually appear within microstructures of one-phase austenitic or ferritic steels starting from the range 60-70% of rolling reduction [9,11]. It should be noted however that well-developed macroscopic shear bands, crossing the entire section or propagating through a considerable thickness of the sheet, were not revealed by TEM observations within the deformed ferrite-austenite microstructure up to relatively high strains (ε =2.3). On the other hand, corrugation of the ferrite-austenite bands visible after 70% and 80% of reduction on micrographs from optical microscopes (Figs. 3c, 11a-b) indicates at macroscopic shearing of two-phase banded structure. Since interphase boundaries are enough strong barriers also for the co-ordinate dislocation motion, therefore by analogy to slip transmission a shear transfer may proceed across the phase interfaces at higher strains and affect changes in microstructure within the bands of both phases. It seems that the structural effects resulting from macroscopic strain localization can not be precisely defined only on the base of morphological features. In the case of significant refinement of a band-like two-phase structure in cold-rolled duplex steels, with a band thickness frequently reduced to less than one micrometer, it is expected that structural features corresponding to macroscopic strain localization manifest themselves in various way depending on chemical composition, SFE value, orientation distribution, deformation conditions, etc. [2,4,6,8].

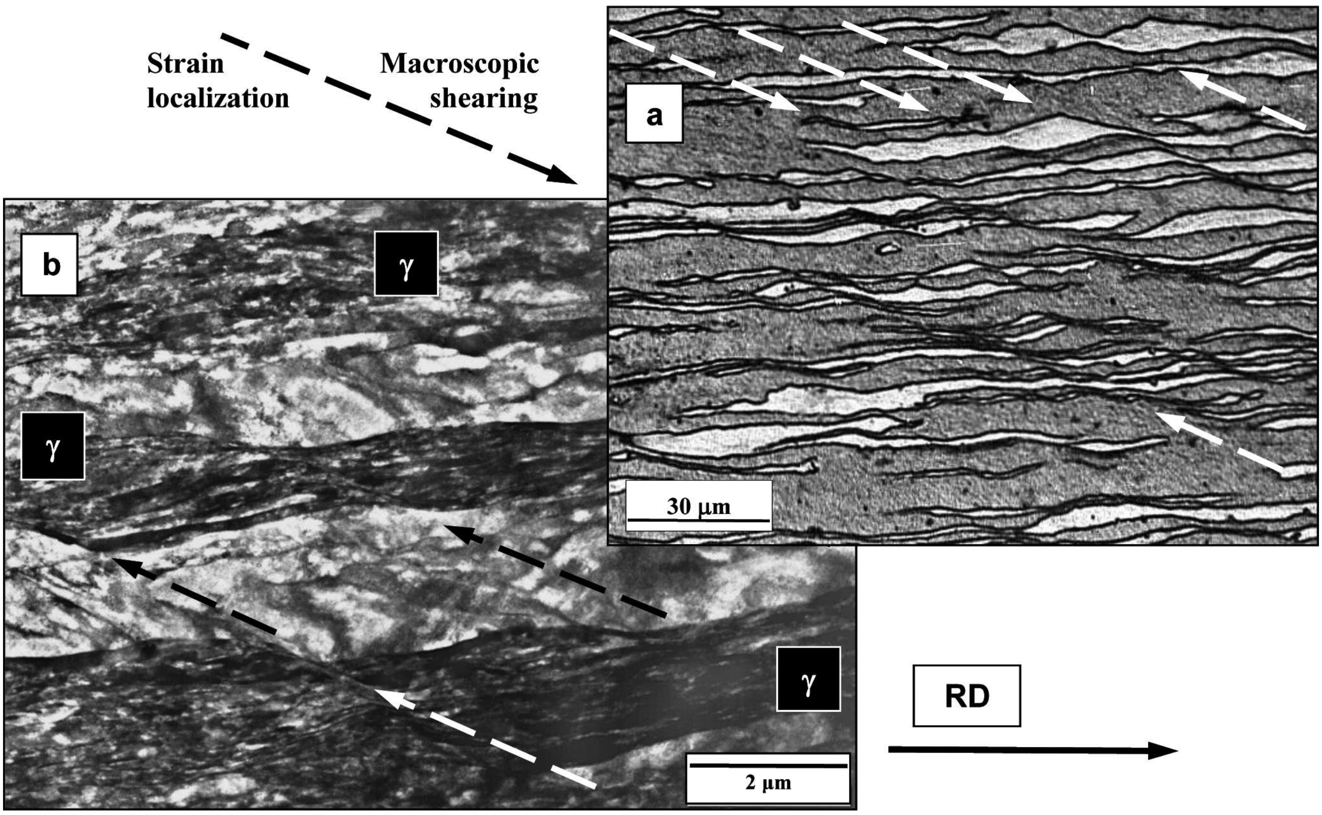

Fig. 11. Strain localization and macroscopic shearing of two-phase microstructure at about 80% of reduction revealed by optical and transmission electron microscopy (**a, b** – respectively)

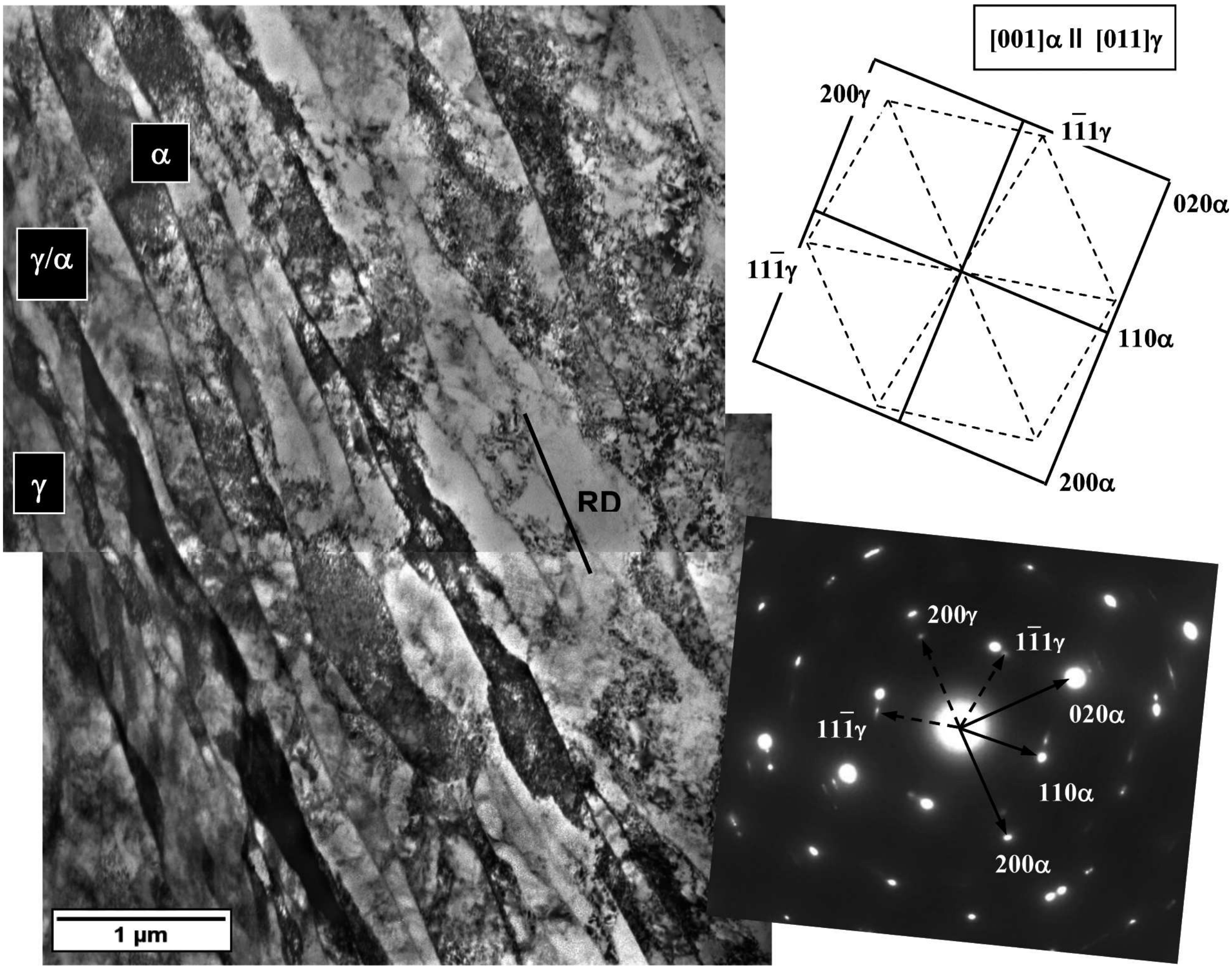

Fig. 12. Partly recovered ferrite microstructures in the form of sub-grains elongated parallel to RD after 80% of rolling reduction

4. Summary

The present research concerns the microstructure evolution and the texture formation in cold-rolled sheets of a model duplex type ferritic-austenitic stainless steel X1CrNi24-6. The thermo-mechanical pre-treatment included forging and solution annealing. Afterwards the steel rods were subjected to cold-rolling within a wide strain range, up to about 90% of reduction (ε =2.3), parallel to the direction of hot-deformation.

The band-like morphology of ferrite and austenite, formed upon processing of examined duplex steel, imposed different conditions for plastic deformation in comparison to one-phase ferritic and austenitic steels. In spite of the fact, that basic mechanisms controlling deformation behavior within the areas of constituent phases occurred essentially the same as in one-phase steels, their appearance and contribution were considerably changed upon deformation of two-phase banded structure.

It should be noted, that co-deformation of the component α- and γ-phases strongly increases strain hardening rate and dislocation density and in consequence forces additional mechanisms, especially at higher strains, in order to accommodate the imposed external deformation. Beside dislocation slip in both phases as well as local shear band formation in γ-phase, the strain induced ($\gamma \rightarrow \alpha$) transformation in austenite and dynamic recovery of ferrite occurred locally at higher strains in areas with increased dislocation density.

The microstructure development within the bands of ferrite and austenite resulted first of all from the following factors: crystallographic structure, chemical composition, stacking fault energy, initial textures and to some extent from interaction between both phases. Basically, the influence of band-like morphology on microstructure evolution resulted from the orientation of the (α/γ) boundaries, which for the most part were parallel to the rolling plane. It turns out, that the phase interfaces are strong obstacles also for the coordinated dislocation motion and hence the structural effects of plastic deformation were usually limited to the areas of both phases. It seems, that the phase boundaries hinder a development of macroscopic shear bands typical for strongly deformed one-phase steels and only a shear transfer is possible across the (α/γ) interfaces, which affects microstructure evolution within the ferrite and austenite bands.

Analysis of the rolling textures in the component α- and γ-phases of examined duplex steel indicates at significant influence of two factors: the specific band-like morphology developed upon processing and the starting orientations after preliminary treatment, on a formation of the ferrite and austenite final textures. To some extent their development in the course of cold-rolling was different in comparison to one-phase ferritic and austenitic steels.

Both constituent phases exhibited specific starting textures after the preliminary treatment, i.e. the {100}<001>cubic and the {110}<001>Goss textures in ferrite and austenite respectively. The texture examination did not reveal any significant orientation changes within the bands of α- and γ-phases up to about 60-70% of deformation. The operation of slip systems in both constituent phases with equal values of relative shear stresses and symmetrical with respect to the (α/γ) interfaces, enabled plastically compatible deformation of ferrite-austenite banded structure without significant lattice rotations.

Visible weakening and spread of the austenite texture as well as considerable changes in the rolling texture of ferrite, observed starting from about 70-80% of reduction, corresponded with the appearance of macroscopic strain localization. Since that strain level the maximum of ferrite texture was shifted from the {100}<001>cubic to the {100}<011>rotated cubic orientation and afterwards into the range {111}<011>to {112}<011>. These orientation changes resulted in a change of the crystallographic relationship between both constituent α- and γ- phases from Bain to K-S orientation relation.

In general, the appearance of structural effects related to macroscopic strain localization and the resulting texture changes within the bands of both component phases were delayed and shifted to higher strains in comparison to one-phase ferritic and austenitic steels. Furthermore, some characteristic texture components were absent or their intensities remained very weak up to high rolling reductions, as in the case of the α_1-fiber (<110>|| RD) and the γ-fiber (<111>|| ND), which are typical fibers for the rolling textures of ferritic steels as well as the alloy type {110}<112>orientation characteristic for austenite rolling textures.

Acknowledgements

The authors would like to thank professor W. Ratuszek and professor A. Korbel for helpful discussions and International Center of Electron Microscopy (IC-EM) AGH-UST for access to TEM equipment. The work was financially supported by the Polish Committee for Scientific Research (KBN) under the contract No. 11.11.110.157.

REFERENCES

[1] J. Keichel, J. Foct, G. Gottstein, Deformation and annealing behavior of nitrogen alloyed duplex stainless steels. Part I: Rolling, ISIJ International **43**, 1781-1787 (2003).
[2] N. Akdut, J. Foct, Microstructure and deformation behavior of high nitrogen duplex stainless steels **36**, 883-892 (1996).
[3] N. Akdut, J. Foct, G. Gottstein, Cold rolling texture development of (α/γ) duplex stainless steel, Steel Research **67**, 450-455 (1996).
[4] J. Hamada, N. Ono, Effect of microstructure before cold rolling on texture and formability of duplex stainless steel sheet, Materials Transactions **51**, 635-643 (2010).
[5] J. Ryś, W. Ratuszek, M. Witkowska, The effect of initial orientation and rolling schedule on texture development in duplex steel, Materials Science Forum **495-497**, 375-380 (2005).
[6] J. Ryś, M. Witkowska, Influence of band-like morphology on microstructure and texture evolution in rolled super-duplex steel, Archives of Metallurgy & Materials **55**, 733-747 (2010).
[7] N. Jia, R. Lin Peng, Y.D. Wang, S. Johansson, P.K. Liaw, Micromechanical behavior and texture evolution of duplex stainless steel studied by neutron diffraction and self-consistent modeling, Acta Materialia **56**, 782-793 (2008).
[8] A. Belyakov, Y. Kimura, K. Tsuzaki, Microstructure evolution in dual-phase stainless steel during severe deformation, Acta Materialia **54**, 2521-2532 (2006).
[9] M. Blicharski, Structure of deformed ferrite-austenite stainless steel, Metal Science **18**, 92-98 (1984).
[10] W. Reick, M. Pohl, A.F. Padilha, Determination of stacking fault energy of austenite in a duplex stainless steel, Steel Research **67**, 253-256 (1996).
[11] D. Raabe, Texture and microstructure evolution during cold rolling of a strip cast and of a hot rolled austenitic stainless steel, Acta Materialia **45**, 1137-1151 (1997).
[12] M. Holscher, D. Raabe, K. Lücke, Rolling and recrystallization textures of bcc steels, Steel Research **62**, 567-575 (1991).
[13] J. Ryś, Compatibility effects at phase interfaces in duplex steel (α/γ) bicrystals, Journal of Materials Processing Technology **64**, 343-352 (1997).
[14] C.W. Sinclair, J.D. Embury, G.C. Weatherly, Basic aspects of the co-deformation of bcc/fcc materials, Materials Science & Engineering **A272**, 90-98 (1999).

Received: 10 February 2012.